

# ESR, SIMS AND TEMF OF AN Y-Ba-Cu-O SUPERCONDUCTOR

I. Kirschner<sup>(1)</sup>, J. Giber<sup>(2)</sup> and I. Halász<sup>(3)</sup>

(1) Department for Low Temperature Physics, Eötvös University, Budapest, Hungary

(2) Department of Atomic Physics, Technical University, Budapest, Hungary

(3) Central Research Institute of Chemistry, Budapest, Hungary

## Abstract

Superconducting transition comes into being between 92 K and 82 K in the samples having a Meissner's state value of 68 vol.%. The main material content has an orthorhombic unit cell of  $Y_1Ba_2Cu_4O_8$  accompanied by low quantity CuO and a sporadic phase. A proof of anisotropic superconductivity, an unusually high  $Cu^{2+}$  ion concentration and a temperature dependent transition of charge carriers have been observed.

## Introduction

On the basis of our earlier research concerned high- $T_c$  superconductivity [1-3], the study of different Y-Ba-Cu-O compounds has been continued in the direction to find out the influence of the exact composition, preparing technique and structure on the superconducting parameters.

In order to accomplish this task, superconducting specimens of the nominal composition of  $Y_1Ba_2Cu_4O_8$  have been prepared for different investigations. The following points of view have played the main role in the sample preparation process:

1. the value of the compatible ionic radii, which has a range of 1.25-1.30,
2. the favourable substitution of yttrium (Y) with alkaline earths (AE)
3. the ratio of (Y+AE) to Cu, which is higher, than 0.5 in these experiments, moreover
4. the redox process and the mixed and variable valence of Cu.

## Characterization of samples

During present investigations SEM, X-ray, resistivity measurement, ESR- and SIMS methods, moreover TEMF experiment have been applied for obtaining information

on the structure and superconducting properties of specimens.

The samples were prepared by solid-state reaction from pure chemicals of  $Y_2O_3$ ,  $BaCO_3$  and  $CuO$  with an appropriate rate. This mixture was pulverized and homogenized by an intensive grinding. The optimum reaction temperature was chosen by a thermogravimetric analysis as a value of  $850\text{ }^\circ\text{C}$  at which the first heat treatment was carried out for 9 h in oxygen atmosphere.

The lined picture obtained by an X-ray Guinier camera with quartz-monochromatized  $CuK_\alpha$  radiation (DRON-2) on the reacted and pulverized mixtures show a fully microcrystalline structure without any amorphous phase.

The powders were then pressed by a pressure of 5 MPa into pellets and then were sintered again at temperature  $850\text{ }^\circ\text{C}$  for 9 h in oxygen atmosphere.

In the course of this preparation process, a slightly distorted, perovskite structure develops without oxygen deficiency.

The photographs taken by a scanning electron microscope (Jeol JXA-50A) on the samples demonstrate a homogeneous microstructure (Fig. 1). The forms of crystals are not sharp, from which a conclusion on a well-sintered state results.

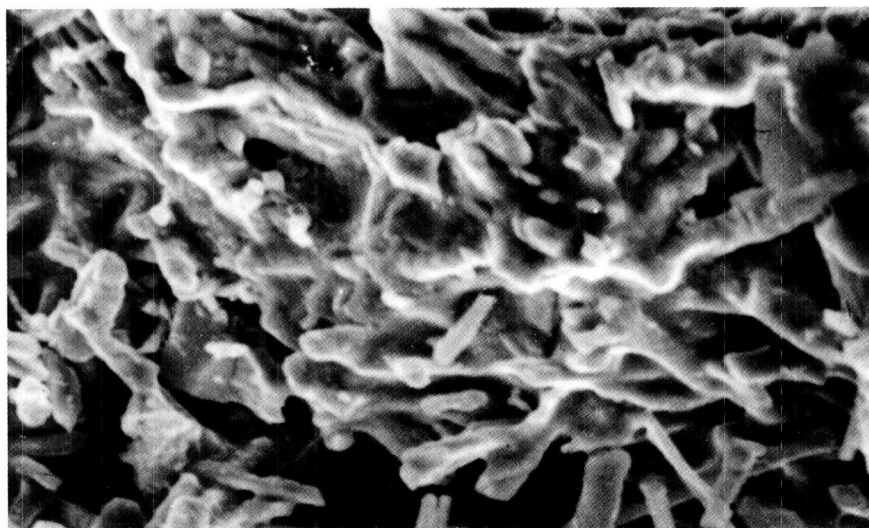


Fig 1. SEM photograph on a sample

The composition of specimens was investigated by X-ray diffraction method (Siemens D-500). This study provides a diffractogram (Fig. 2), demonstrating a nearly single-phase material having a main phase of  $Y_1Ba_2Cu_4O_8$  and other compositions only in very low quantity. The majority phase of stoichiometry of  $Y:Ba:Cu=1:2:4$  has an orthorhombic symmetry with lattice parameters  $a=3.83\text{ \AA}$ ,  $b=3.88\text{ \AA}$  and  $c=27.22\text{ \AA}$

and this is responsible for the superconductivity. The minority phase is the well-known Cu-O of monoclinic unit cells. Finally, the peaks, which can not be indexed indicate the existence of an unidentified sporadic phase.

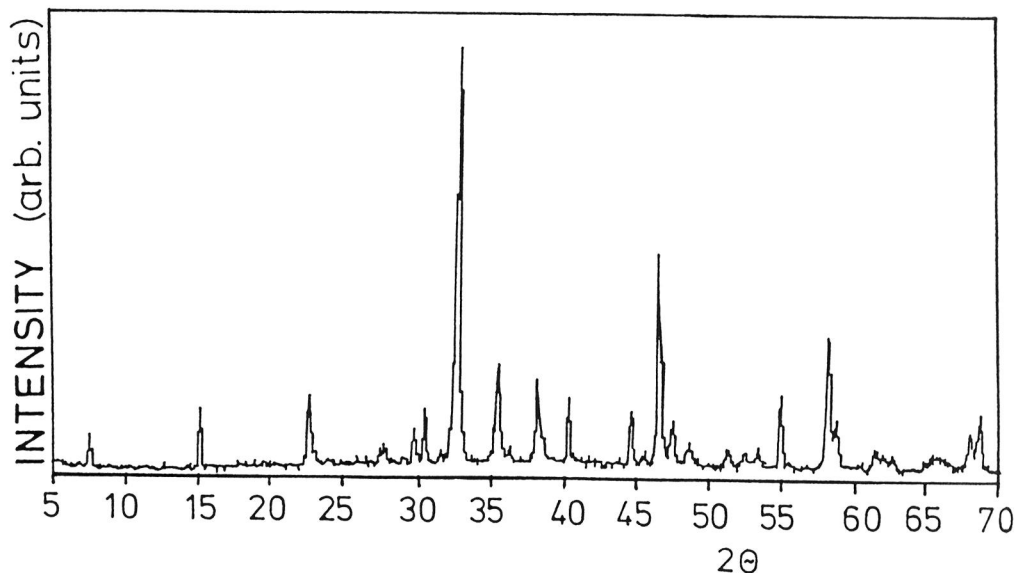


Fig 2. X-ray diffractogram of a sample

Since the (1,2,4) compound is an oxygen stoichiometric one [4], the number of oxygen atoms practically can not be changed. Therefore the lattice parameters determined by double Cu-O chains can also not easily be varied by substitution of other atoms. From this the higher thermal stability of the oxygen content follows, as compared to the (1,2,3) phase. As the experiments show, this statement is, however, valid only until a given temperature, and in the range above 850 K the (1,2,4) phase decomposes into (1,2,3) one and CuO.

### Superconducting properties

The dependence of the resistance  $R$  on temperature  $T$  was determined by a conventional four-probe technique using evaporated gold contacts on the samples to which the electrical leads were soldered by silver paste. A typical  $R$ - $T$  characteristic is shown in Fig. 3. The specimens show metallic behaviour in the whole temperature interval under investigation, having room temperature specific resistivity of  $\rho_{300}=8\text{-}11\text{ m}\Omega\text{cm}$ . As it can be seen, the sharp drop of the resistance starts at 92 K and zero-resistivity state sets in at 82 K.

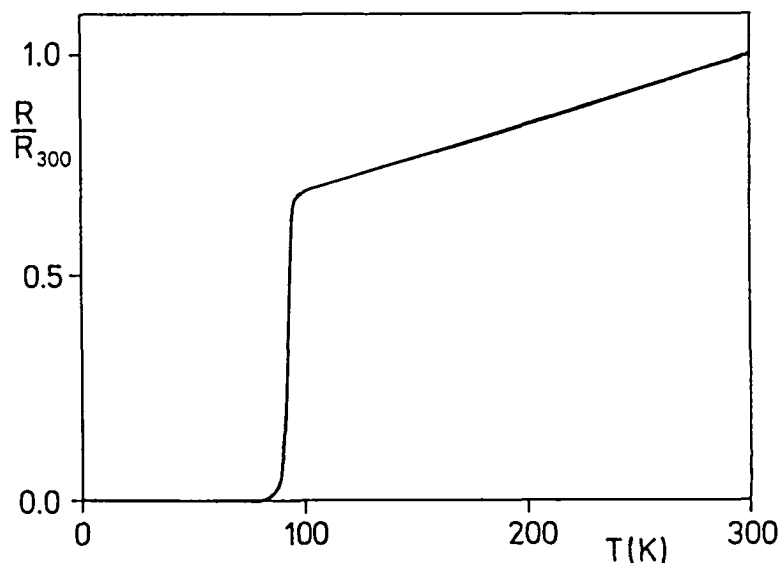


Fig 3. Dependence of the resistance on temperature of a sample

Double-coil dynamic magnetic measurements were performed on the samples forming prism of dimensions  $2 \times 2 \times 12 \text{ mm}^3$ . During these experiments an a.c. method was used in the frequency range of 5-150 kHz and at effective magnetic field interval of 0.1-27 Oe. As the investigation shows,  $68 \pm 4$  vol. % of samples material is in pure Meissner's state at low temperatures (Fig. 4).

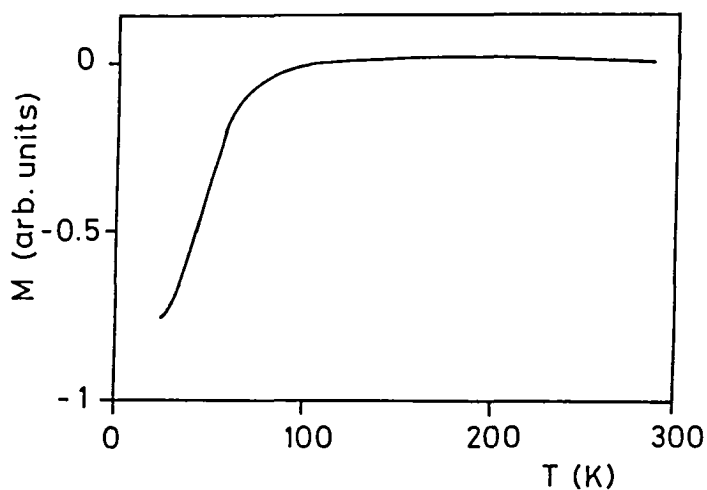


Fig 4. Typical a.c. susceptibility curve at 100 kHz

Superconducting transition has also been traced with an X-band (9.5 GHz) Electron Spin Resonance (ESR) equipment (ERS 200). ESR investigation hints at a strongly anisotropic and layered structure of the specimens. Above the temperatures of

dropping resistance, the samples have an ESR signal of asymmetrical shape (Fig. 5).

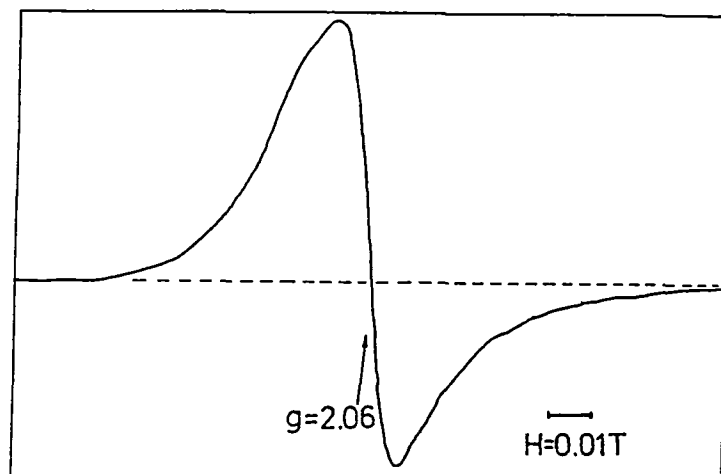


Fig 5. ESR signal of a sample

The center of the line corresponds to the gyromagnetic factor with average value of  $g=2.06$  and its peak to peak width is 152 Oe. The shape of the signal slightly depends on the angle between pressing plane and direction of the magnetic field, thus it refers to an anisotropy in the samples and a tensorial character of  $g$ , which survives the pulverizing of the specimens.

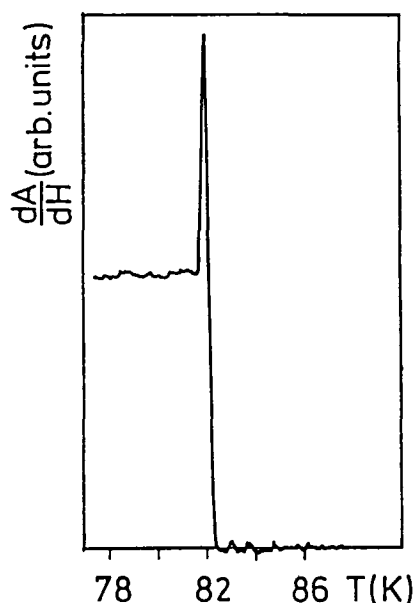


Fig 6. Temperature dependence of the derivative of microwave absorption near  $T_c$ .

During the transition to zero-resistivity state a sharp increase in the base-line level occurs at 82 K, although the ESR signal remains unchanged. The increase of the base-line level decreases with the static magnetic field.

This indicates a magnetic field dependent microwave absorption  $A$ , which is related to the dissipative behaviour of type II superconductivity of high- $T_c$  superconductors. Figure 6 shows the temperature dependence of the first derivative of microwave absorption on static magnetic field near the zero-resistivity state. It demonstrates a drastic change in the absorption properties at the critical temperature, which reflects the transformation of the state in samples.

Detailed experimental investigation was carried out on the specimens by Secondary Ion Mass Spectroscopy (SIMS, type Balzers). Dynamic spectra were measured in argon and oxygen atmosphere at a monitor current of  $1 \times 10^{-6}$  A in a wide mass range. Fig. 7 and 8 show the positive and negative secondary ion spectra, respectively, taken on the characteristic mass range of 1 - 100 in argon atmosphere, where the peaks of main components and micro-impurities can be seen. In the higher mass range  $YO^+$ ,  $BaO^+$ ,  $Ba_2O^+$  molecule ions and  $Dy^+$ ,  $Yb^+$ ,  $Pt^+$  impurity ions appear as well.

According to the observation, the oxygen atmosphere increases the peak of  $Y^+$  4.7- times,  $Ba^+$  2.1- times and  $Cu^+$  3.5-times, indicating that the original material is not completely oxidized. This result is in agreement with earlier statement on oxidation state.

The existence of the high intensity  $Cu^-$  peak compared to the  $Cu^+$  one, may be a very important point explaining the superconducting behaviour of this compound. The  $Cu^+/Cu^-$  ratio being here  $10^{-1}$  is quite unusual comparing to the value of  $10^2$  in copper oxides and  $2 \times 10^2$  in copper alloys. (Similar effect for metallic components was found only at noble metals, namely at Au and Pt). From this fact a significant interaction between Cu ions and electrons can be supposed, due to which the Cu atoms leaving the bulk material are surrounded by an excess electronic cloud. It means that less electrons can take place in the transport and so a positive charge carrier conductivity may occur. This supposition was controlled by TEMF measurement too.

Thermoelectric effect can also be detected in the granular and anisotropic superconductors creating a temperature difference between two sides of samples [5].

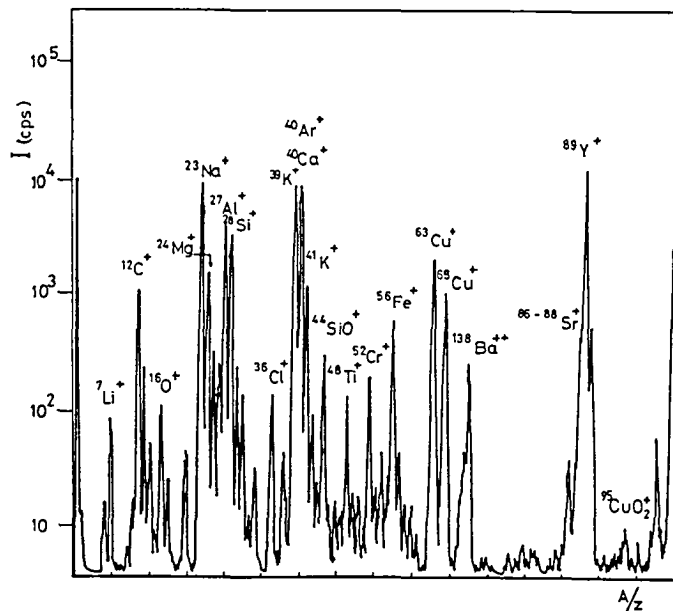


Fig 7. A positive SIMS spectrum of a sample with 3 keV  $\text{Ar}^+$  bombardment (A=mass number, Z=particle charge number)

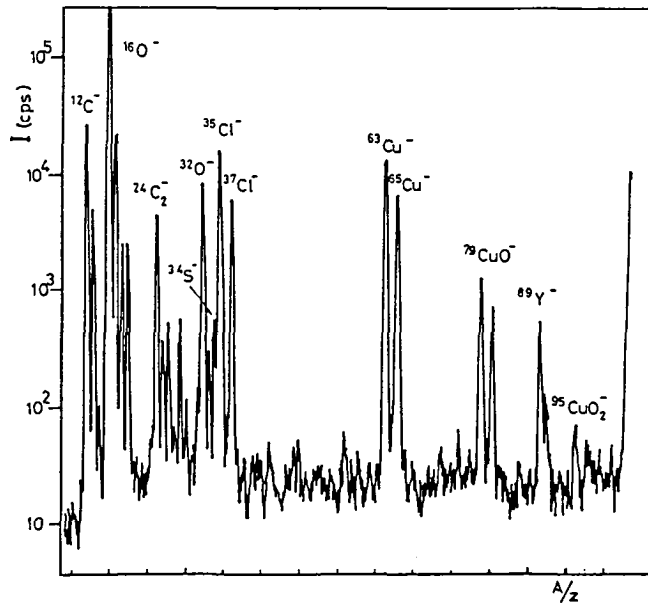


Fig 8. A negative SIMS spectrum of a samples with 3 keV  $\text{Ar}^+$  bombardment (A=mass number, Z=particle charge number)

As Fig. 9 shows, the thermoelectric voltage has a negative sign and a slightly increasing tendency in its absolute value during the cooling stage without any external magnetic field in the temperature interval of 220-124 K. Below this temperature the TEMF is decreasing and reaches zero value at 82 K. After the zero value it has an increasing and later a decreasing branch of positive sign and ceases at about 50 K.

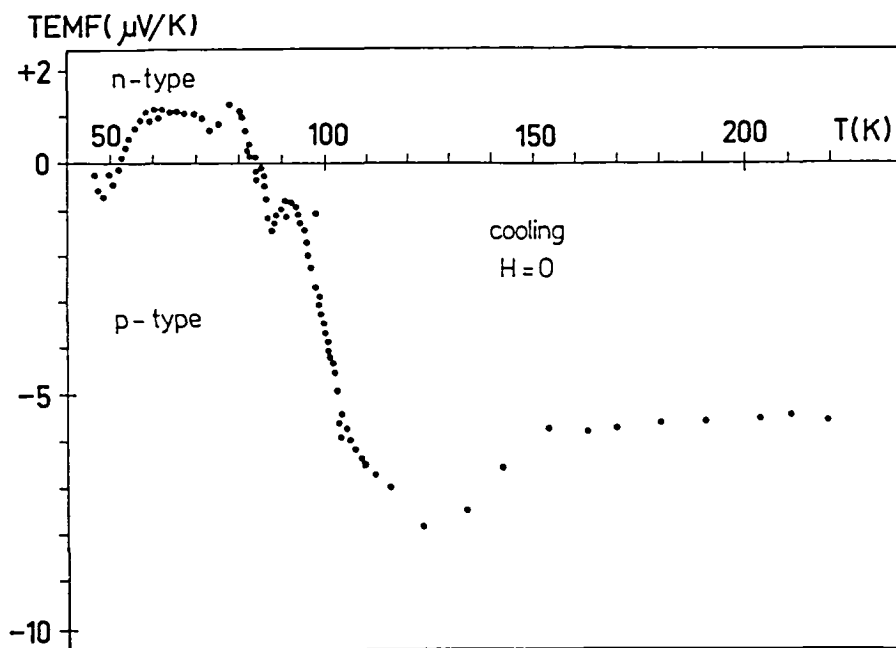


Fig 9. Dependence of TEMF on the temperature in the cooling stage without magnetic field

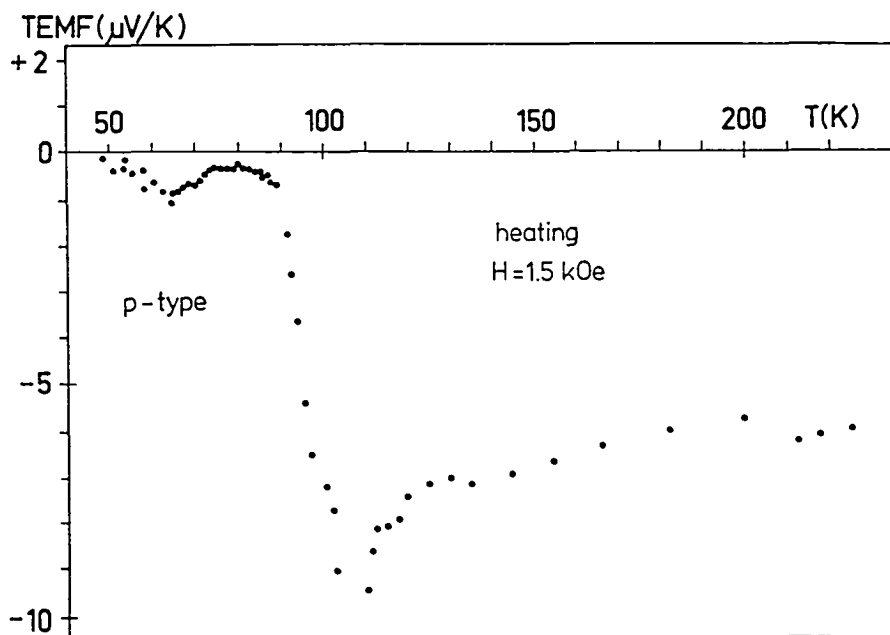


Fig 10. Dependence of TEMF on the temperature during heating process in an external magnetic field

Investigating this phenomenon during the heating stage in an external magnetic field of 1.5 kOe, the sign of TEMF is negative in the whole temperature range (Fig. 10).

Starting from 50 K, the curve of TEMF firstly has an increasing character in its absolute value until 110 K. At this point a sharp break then a moderate decrease and a saturation tendency in the investigated temperature interval (until 220 K) can be observed.

If a temperature gradient exists in the sample between two opposite surfaces, the charge carriers diffuse from higher-temperature side to the lower-temperature one until a stationary voltage difference established. In the case of p-type charge carriers the cold surface will be more positive and in the presence of n-type ones, more negative. This phenomenon represents a positive-negative transition of the charge carriers occurring at the temperature of zero-resistivity state. In contrast with this observation there is no change in dominant carriers during the heating stage in an applied external magnetic field.

Comparing the magnitude of the effect in other materials, the obtained voltage signals are generally higher, than those for metals and lower, than the thermal voltages belonging to semiconductors. The obtained TEMF values were independent from the materials (bronze, copper or nickel) of the measuring electrodes.

In consequence of granular and porous character of the high- $T_c$  oxide superconductors a spatial fluctuation of the chemical potential and a phonon drag appear, which play together an important role in the formation of TEMF-curve at low temperatures (below 124 K), but they alone can not change the sign of thermoelectric voltage. In this way, the results of these experiments refer to a complicated mechanism, due to that the holes, the  $p \leftrightarrow n$  transition and the electrons are together responsible for establishing superconductivity [6].

Thermoelectric voltage is affected by the relatively large electron-phonon interaction and the creation of superconducting pairs counteracts the diffusion of electrons (and so the thermoelectric effect), therefore a decrease of the absolute value of TEMF can be observed at low temperatures. In this way, the maximum of the positive branch is much smaller, than the values of the negative branch at higher temperatures, but it shows that the pairing process is not capable to cease fully the thermoelectric voltage in anisotropic superconductors in the transitional range.

Finally, we would like to point out, that this phenomenon can be explained in the framework of Ginzburg-Landau theory [7]. If, the power series of the superconducting free energy is completed by a new term, the Ginzburg-Landau equations will be able to imply the thermodynamic cross-effects, namely the thermoelectricity too.

## Conclusions

From the analysis of recent investigation some conclusions can be drawn:

1. Relatively low temperatures of the heat treatment can result in nearly single phase Y-(1,2,4) of reproducibility and long time stability.
2. Specific effects which can be detected by non-conventional methods of research can contribute to the explanation of the mechanism of high- $T_c$  superconductivity in different compound.

## References

1. I.Kirschner, J. Bánkuti, M. Gál and K. Torkos, Phys. Rev. **B36**. 2313. (1987).
2. R. Laiho, E. Lähderanta, L. Säisä, Gy. Kovács, G. Zsolt, I. Kirschner and I. Halász, Phys. Rev. **B42**. 347. (1990).
3. A. C. Bódi and I. Kirschner, Phys. Lett. **A181**. 479. 1993.
4. J. Karpinski, S. Rusiecki, E. Kaldis, B. Bucher and E. Jick, Physica **C160**. 449.(1989).
5. A. Mawdsley, H. J. Trodahl, J. Tallon, J. Sarfati and A. B. Kaiser, Nature **328**. 233. (1987).
6. T. Porjesz, T. Kármán, I. Kirschner, Gy. Kovács, G. Zsolt and H. Beyer, ICTP Report 87-278k, Trieste, 1987.
7. V. L. Ginzburg and L. D. Landau, Zh. Exp. i Teor. Fiz. **20**. 1064. (1950).